IOP Publishing Nanotechnology
Nanotechnology **25** (2014) 094006 (12pp) doi:10.1088/0957-4484/25/9/094006

A low cost, safe, disposable, rapid and self-sustainable paper-based platform for diagnostic testing: lab-on-paper

M N Costa[1], B Veigas[1,2], J M Jacob[1], D S Santos[1], J Gomes[3], P V Baptista[2], R Martins[1], J Inácio[3] and E Fortunato[1]

[1] CENIMAT/I3N, Departamento de Ciência dos Materiais, Faculdade de Ciências e Tecnologia, Universidade Nova de Lisboa, Campus de Caparica, 2829-516 Caparica, Portugal
[2] CIGMH, Departamento de Ciências da Vida, Faculdade de Ciências e Tecnologia, Universidade Nova de Lisboa, Campus de Caparica, 2829-516 Caparica, Portugal
[3] Instituto Nacional de Investigação Agrária e Veterinária, I.P. (INIAV, I.P.), Unidade Estratégica de Investigação e Serviços em Produção e Saúde Animal, Lisboa, Portugal

E-mail: joao.inacio@iniav.pt and emf@fct.unl.pt

Received 5 August 2013, revised 12 September 2013
Published 12 February 2014

Abstract

There is a strong interest in the use of biopolymers in the electronic and biomedical industries, mainly towards low-cost applications. The possibility of developing entirely new kinds of products based on cellulose is of current interest, in order to enhance and to add new functionalities to conventional paper-based products. We present our results towards the development of paper-based microfluidics for molecular diagnostic testing. Paper properties were evaluated and compared to nitrocellulose, the most commonly used material in lateral flow and other rapid tests. Focusing on the use of paper as a substrate for microfluidic applications, through an eco-friendly wax-printing technology, we present three main and distinct colorimetric approaches: (i) enzymatic reactions (glucose detection); (ii) immunoassays (antibodies anti-*Leishmania* detection); (iii) nucleic acid sequence identification (*Mycobacterium tuberculosis* complex detection). Colorimetric glucose quantification was achieved through enzymatic reactions performed within specific zones of the paper-based device. The colouration achieved increased with growing glucose concentration and was highly homogeneous, covering all the surface of the paper reaction zones in a 3D sensor format. These devices showed a major advantage when compared to the 2D lateral flow glucose sensors, where some carryover of the coloured products usually occurs. The detection of anti-*Leishmania* antibodies in canine sera was conceptually achieved using a paper-based 96-well enzyme-linked immunosorbent assay format. However, optimization is still needed for this test, regarding the efficiency of the immobilization of antigens on the cellulose fibres. The detection of *Mycobacterium tuberculosis* nucleic acids integrated with a non-cross-linking gold nanoprobe detection scheme was also achieved in a wax-printed 384-well paper-based microplate, by the hybridization with a species-specific probe. The obtained results with the above-mentioned proof-of-concept sensors are thus promising towards the future development of simple and cost-effective paper-based diagnostic devices.

(Some figures may appear in colour only in the online journal)

1. Introduction

The World Health Organization established guidelines for the development of diagnostic tests suitable for point-of-care applications, which are summarized under the acronym ASSURED (affordable, sensitive, specific, user-friendly, rapid and robust, equipment-free and delivered to those in need) [1]. Such diagnostic tests are in high demand, targeting diseases such as tuberculosis and leishmaniasis, mainly in the developing world, where they remain major impoverishment factors for local communities. Currently, there is a strong interest in the use of biopolymers in the electronic and biomedical

industries, towards low-cost applications (such as ASSURED diagnostic tests).

Cellulose is the Earth's most abundant biopolymer and it is of tremendous global economic importance. This natural polymer represents about one-third of plant tissues and can be restocked by photosynthesis. For industrial use, cellulose is mainly obtained from wood pulp and cotton and it is mostly used to produce cardboard, paper, and to a smaller extent converted into a wide variety of derivative products such as cellophane and rayon. Both cellophane and rayon are known as 'regenerated cellulose fibres'. Cellulose is also the raw material in the manufacture of nitrocellulose (cellulose nitrate) that was historically used in smokeless gunpowder and as the base material of celluloid, used in photographic and movie films until the mid 1930s. Nitrocellulose was used for the first time as a solid support for diagnostic assays in 1963 for the recognition of RNA–DNA complexes [2]. The possibility of improving the competitiveness in existing materials and developing entirely new kinds of products is of current interest, in order to enhance and to add new functionalities to an abundant and renewable material. One of these novel applications of cellulose is the so-called 'Bioactive Paper' [3]. Under this concept, simple, portable, disposable, and inexpensive paper-based sensors are proposed, allowing us to run multiple bioassays simultaneously. Bioactive paper is a low-cost and easy-to-use product modified with biologically active chemicals, enabling the detection of pathogen markers (e.g. *Escherichia coli* and *Salmonella* spp., *Mycobacterium tuberculosis*, and *Leishmania*) in both human health and veterinary settings. Other promising applications for bioactive paper range from food packaging and hospital masks to paper strips for detecting and purifying unsafe drinking water or checking for banned pesticides in crop produce, amongst others.

In 2007, a landmark study of the Whitesides group at Harvard University introduced paper-based microfluidic devices as an inexpensive platform that may potentially meet all ASSURED requirements [4, 5]. The concept of using cellulose/paper as a support for developing value-added diagnostic devices is very attractive and challenging. Paper matrices are inexpensive, readily available with various formats/properties, and their natural porous structure is amenable to lateral flow assays [1]. With paper-based devices, simultaneous and independent multi-analyte assays can be conducted that do not require the use of pipettes, syringes, needles, pumps or electric energy [5]. The devices are based on the definition of microchannels on hydrophilic paper via the patterning of walls of hydrophobic polymers, photoresist or wax [5, 6]. Multiple detection zones for different target compounds are created by deposition of reagents on the paper surface (e.g. enzymes, antibodies) [1]. Three-dimensional networks of channels can be fabricated by stacking alternating layers of patterned paper and double-sided adhesive tape with holes [4, 7], as well as fully enclosed 2D paper devices [8]. The movement of liquid samples within the channels is governed by capillarity. When the sample reaches the detection zone, a reaction occurs and a colorimetric or, for example, an electrochemical detection system signals the reaction [9–12]. Assays for the detection of total proteins, cholesterol and glucose in fluids have already been demonstrated and more specific biorecognition assays usually involve antibody–antigen interactions [1, 4, 6].

Several methods are available for patterning paper, with different costs and resolutions. Photolithography with hydrophobic photoresist or inkjet-printing with polydimethylsiloxane (PDMS) were described, but these methods usually suffer from complex fabrication processes or high cost [1, 5]. The most promising technology for large-volume paper patterning uses a solid wax printer to print the sensors' layout in solid hydrophobic wax [4, 6]. The printed paper is then processed using a hot plate or an oven, a procedure that will enable the wax to melt and diffuse vertically through the porous paper, creating hydrophobic barriers that define hydrophilic channels, fluid reservoirs and reaction zones. However, paperfluidics is at an early stage of study, development and field application. Amongst other hurdles, the methods for mass patterning and immobilizing more delicate biomolecules such as antibodies/antigens, nucleic acid probes or enzymes on the paper matrices are still in an immature state. The stability of biomolecules on paper surfaces during short and long-term storage needs to be assessed, and the currently described biorecognition assays usually lack sensitivity [1, 3, 4]. Paper surface chemistry (e.g. the presence of wet-strength resins) and porosity influence the immobilization of biomolecules. Although paper made from pure cellulose is usually not considered an ideal substrate for immobilization, different approaches have been proposed to accomplish this: (i) physical adsorption (simple but biomolecules can be easily washed off) [3, 10]; (ii) chemical coupling, where biomolecules are anchored to the paper surface via covalent bonds (involving multiple chemical steps) [3, 13]; (iii) biochemical coupling using, e.g., carbohydrate binding modules (CBMs) [3]; (iv) bioactive pigments, where biomolecules are coated on colloidal particles that are then inkjet-printed or spotted onto the paper, where they remain immobilized due to mechanical entrapment [14]. A large expansion of the paperfluidics field is expected in coming years due to the increasing support from non-profit companies and foundations. Figure 1 presents the three main microfluidic technologies: (i) SU8/PDMS lithography, (ii) embossing, and (iii) paperfluidics/lab-on-paper.

In this work we present our results towards the development of paper-based microfluidics for molecular diagnostic testing. Paper properties were evaluated and compared to nitrocellulose, the most commonly used material in lateral flow and other rapid tests. Focusing on the use of paper as a substrate for microfluidic applications, through an eco-friendly wax-printing technology, we present three main and distinct colorimetric approaches: (i) enzymatic reactions, (ii) immunoassays, and (iii) nucleic acid sequence identification. All of the generated knowledge will be applied towards the assembly of point-of-care diagnostic prototypes, capable of being globally used.

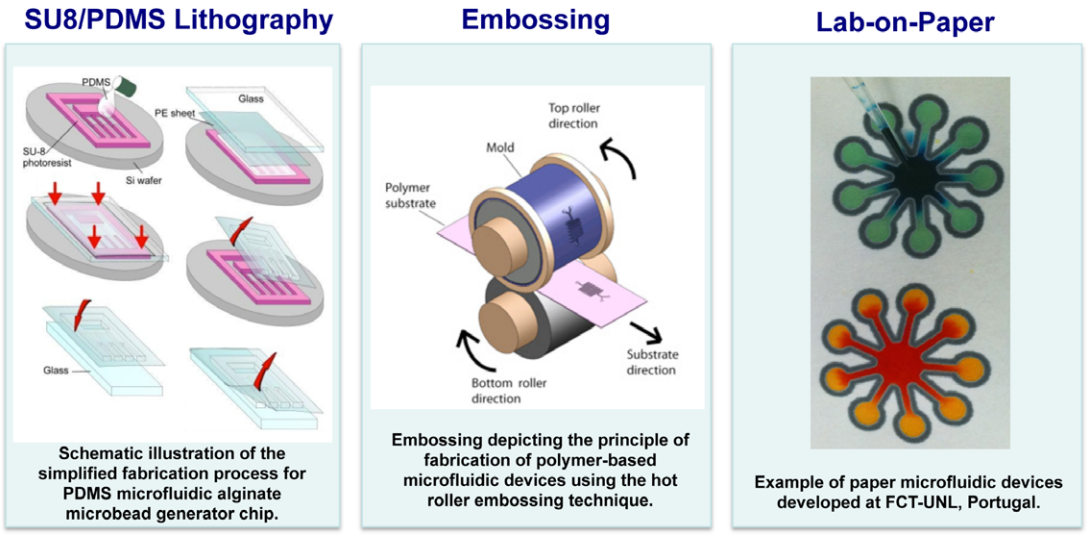

Figure 1. Illustration of the main microfluidic technologies. The complexity/cost decreases from left to right.

2. Paper: an ideal material for bioassays?

Paper has been used in the analytical laboratory since the beginning of the 20th century, especially for filtration purposes. However, the most significant increase in the use of this material started with the discovery by Martin and Synge, to whom the Nobel Prize was awarded in 1952, for the invention of 'paper chromatography'. Cellulose-based materials, such as paper, are compatible with biological samples, can be chemically modified to incorporate functional groups, and are a good medium for colorimetric tests, since they can provide a white background. From the perspective of paperfluidics application, critical properties include paper surface chemistry, porosity and optical properties. Surface chemistry and porosity influence the immobilization of biomolecules (e.g. antibodies and oligonucleotides) as well as fluid wicking [3]. Knowledge of the paper's optical properties is also critical, due to their importance in unfolding the test results. Colorimetric detection is probably the most suitable option for this type of device, since results can be read by the naked eye without the use of additional equipment.

Historically, nitrocellulose was used for the first time as a solid support in diagnostic assays in 1963 for the recognition of RNA–DNA complexes [2]. The breakthrough related to this technique came from Southern's discovery in 1975 where he found that nucleic acids could be transferred from an agarose gel to nitrocellulose [15]. In fact due to the importance of this discovery, the method is named the 'Southern blot'. Since then nitrocellulose has become very popular for a large variety of blotting techniques, in biological research and clinical tests, due to the unique ability to interact with the three main classes of biomolecules: proteins, DNA and RNA [16].

Nitrocellulose is obtained by the reaction of cellulose with nitric acid, replacing the cellulose hydroxyl groups with nitrate groups (NO_2). This is clearly observed from Fourier transform infra-red spectroscopy (FTIR), where we can see the substitution of the OH groups by the nitrate groups

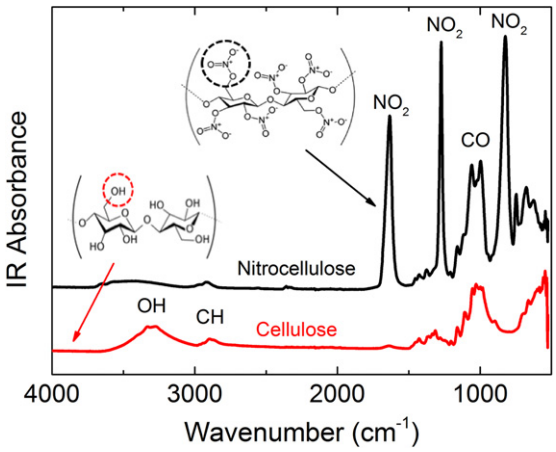

Figure 2. FTIR spectra of chromatography paper (Whatman no. 1) and nitrocellulose (Whatman BA85 Protran) at room temperature. The inset presents the molecular structures of both materials.

(figure 2). Three intense bands, due to the different vibrations of the nitrate group, are observed at around 1660 cm^{-1} (antisymmetric NO_2 stretching), 1280 cm^{-1} (symmetric NO_2 stretching), and 840 cm^{-1} (valence NO stretching) [17]. Comparing cellulose and nitrocellulose FTIR spectra, another change is visible in the frequency range between 3400 and 3500 cm^{-1}, a decrease in the intensity corresponding to the OH group.

Since the first attempt at biomolecule immobilization on nitrocellulose, a great deal of work has been done in order to understand the real mechanism as well as the theory behind immobilization, but until today, the exact interaction is not fully understood [18]. Nevertheless, there are some hypotheses: (i) there is a hydrophobic interaction between the carbon-containing nitrocellulose and the hydrophobic part of the biomolecule, and/or (ii) the existence of an electrostatic interaction between the dipoles of nitrocellulose nitrate groups and the dipoles of the biomolecules [16, 19].

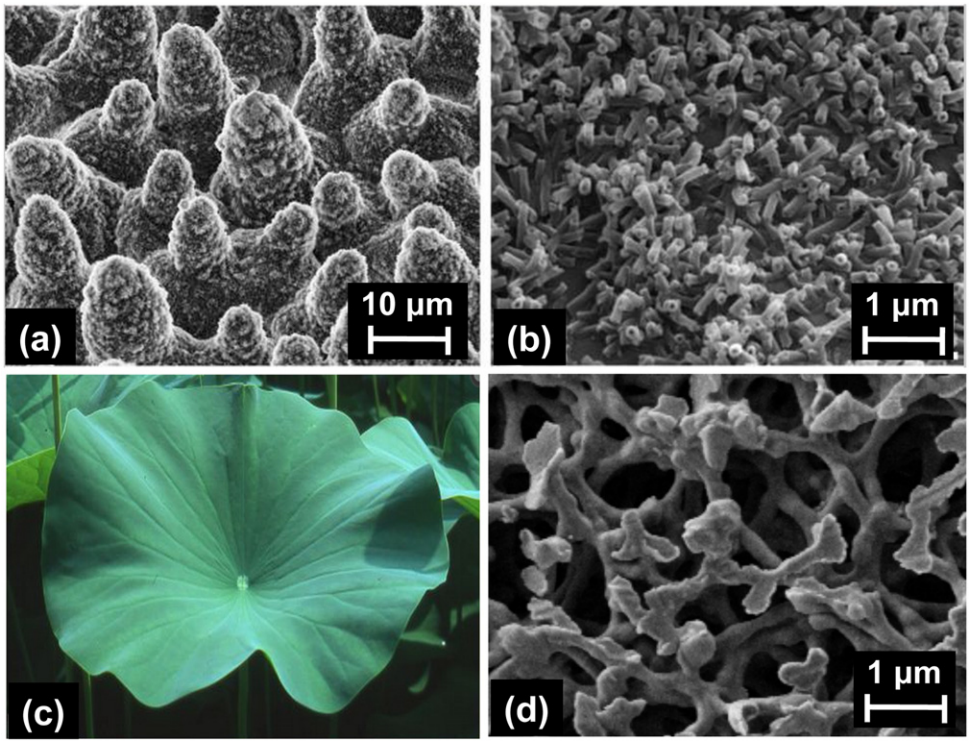

Figure 3. (a) Scanning electron microscopy of a Lotus leaf microstructure and (b) a Lotus leaf nanostructure; (c) Lotus leaf and (d) Whatman BA85 Protran nitrocellulose nanostructure.

In terms of surface properties, nitrocellulose is hydrophobic, and membranes made from nitrocellulose do not wet in water. It is well known that one way to increase the hydrophobic properties of a surface is by increasing surface roughness [20]. This is a similar effect to that observed in nature, where plants make use of fascinating nanoscale surface properties to remain clean in dirty environments. An example of this is the Lotus plant (figure 3), which is considered the 'holy-grail' of natural self-cleaning systems. The surface of the Lotus leaf exhibits a complex structure that incorporates both nano- and micro-scale roughness. The plant's self-cleaning mechanism arises from a combination of multiple-length roughness and inherent hydrophobicity. Figure 3 compares the Lotus leaf, adapted from Ensikat *et al* [21], with the nitrocellulose surface (using the same magnification), where it is possible to see the same type of nanostructure that enhances the hydrophobicity. The hydrophobic rough surface induces a higher contact angle, forcing water droplets to sit on the apex of the rough structures [20].

To produce membranes that are wettable, manufacturers add a surfactant as a component of the lacquer or apply it to the membrane at the end of the casting process [18]. Concerning surface properties, specifically wettability, paper presents an advantage over nitrocellulose, since it is hydrophilic in nature and does not require additional processing steps. In order to compare the surface morphology of nitrocellulose and cellulose-based paper, figure 4 shows their microstructures obtained by scanning electron microscopy. It is clear that besides having a completely different microstructure, chromatography paper Whatman no. 1 has a higher porosity (∼68%) with a corresponding higher pore diameter (100 μm) than nitrocellulose Whatman BA85 Protran (∼0.45 μm), to which corresponds a much lower contact angle, of 12° (result not shown).

Whatman paper is manufactured from high quality cotton linters, which have been treated in order to achieve a high alpha cellulose content (>98%) to guarantee quality, reproducibility, and uniformity. Cellulose is a polymer made up of a long chain of glucose molecules linked by oxygen bridges. Cotton cellulose differs from wood cellulose primarily by having a higher degree of polymerization and crystallinity. Crystallinity indicates that the fibre molecules are closely packed and parallel to one another (as illustrated in the inset of figure 5). From the data presented in figure 5, it is possible to qualitatively evaluate that Whatman paper has a typical semi-crystalline cellulose structure, which is corroborated by the characteristic diffraction peaks at $2\theta =$ 14.7°, 16.8° and 22.7° corresponding to the $(1\bar{1}0)$, (110) and (200) crystallographic planes of monolithic cellulose type I, respectively (PDF files: 00-056-1717, 00-056-1718 and 00-056-1719), with a degree of crystallinity of 86% [22]. In contrast, nitrocellulose shows an amorphous structure corroborated by the absence of diffraction peaks as well as by the random structure exhibited in figure 4.

Although nitrocellulose has been widely used for biological and clinical assays, it is not an ideal matrix for lateral flow devices. It does have certain amenable characteristics, such as high protein-binding capacity and capillary flow properties, and it is available in a variety of products with

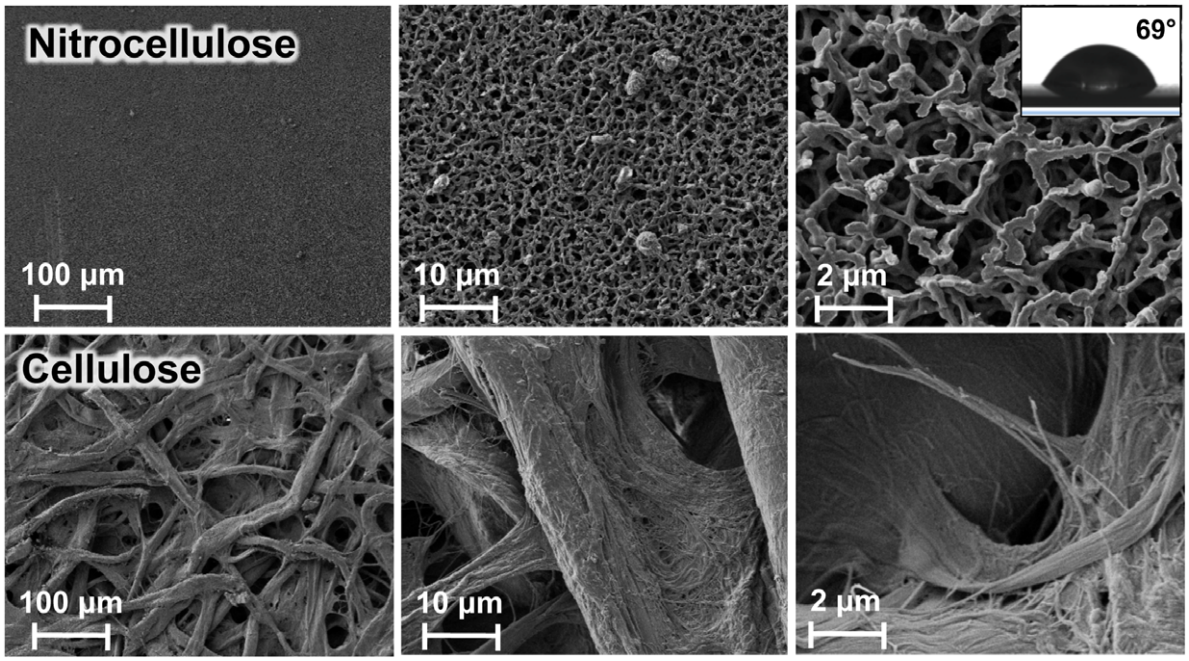

Figure 4. Scanning electron microscopy of nitrocellulose Whatman BA85 Protran (upper part) and chromatography paper Whatman no. 1 (lower part) with three different magnifications. The inset shows the water contact angle for nitrocellulose.

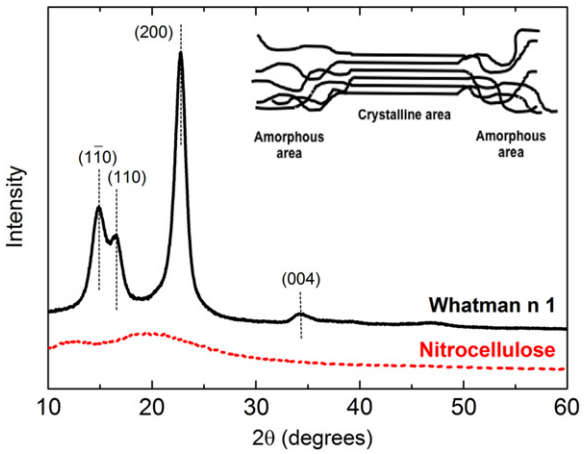

Figure 5. X-ray diffraction (XRD) of chromatography paper Whatman no. 1 and nitrocellulose Whatman BA85 Protran. The inset shows schematically the amorphous and crystalline areas of cellulose.

varying wicking rates and surfactant contents. However, it is a highly flammable material, expensive when compared to paper, and presents low mechanical properties (brittle), which make it difficult to handle, and to pattern [18]. Cellulose-based paper does not have these disadvantages and has the ideal properties for the development of point-of-care colorimetric diagnostic platforms.

3. Lab-on-paper technology

Lab-on-paper technology was introduced in 2007 by the Whitesides group and is achieved by the definition of microchannels on hydrophilic paper via patterning with hydrophobic polymers, photoresist or wax [5, 6]. In this work we have optimized the design of microfluidic networks and the respective paper patterning procedures using wax-printing technology. This approach uses a solid ink printer, in which the ink is supplied as solid wax that is melted before being ejected from the print head and solidifies immediately on the paper surface. This is an innovative, award-winning colour printing technology available only from Xerox. The technology generates up to 90% less printing waste than comparable colour laser printers, because there are no cartridges to dispose of and less packaging to add to landfills. Solid ink is formulated from a non-toxic resin-based polymer and is safe to handle. It is made of a mixture of hydrophobic carbamates, hydrocarbons and dyes that melts at 80 °C, being suitable for piezoelectric printing.

The printed paper is processed on a hot plate (140 °C, 2 min), allowing the wax to diffuse vertically through the porous paper, creating hydrophobic barriers that define hydrophilic channels and reaction zones (figure 6). Fully enclosed 2D paper devices were made simply by printing a superficial layer of wax, which can incorporate a colour scale and other relevant information. The patterned paper was also used in the fabrication of 3D microchannel networks (figure 7(a)), stacking alternating layers of paper and double-sided adhesive tape with holes, filled with cellulose powder, ensuring the connection between the hydrophilic channels in adjacent layers. Device encapsulation is extremely important for diagnostic tests since it protects the channels and reagents from contamination and degradation, contains the fluids within the channels so that the devices can be manipulated more easily, and also reduces fluid evaporation [8]. Because paper is a relatively resistant material, paperfluidics encapsulation dispenses with plastic casings and can be done simply by

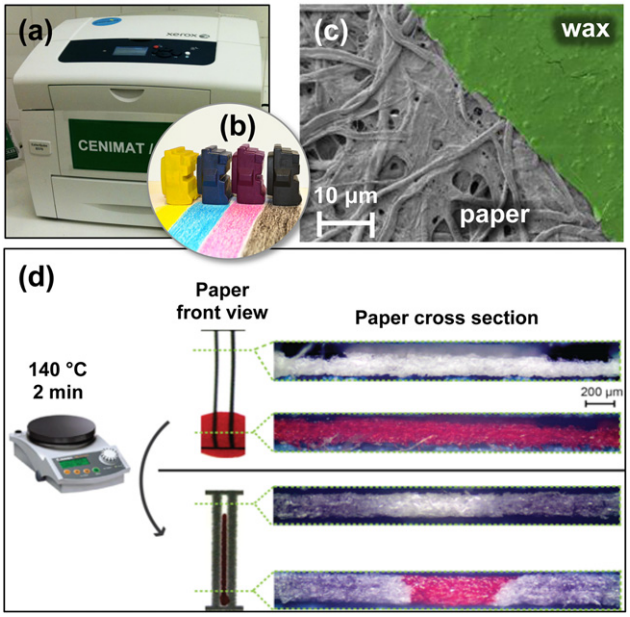

Figure 6. Schematics of the lab-on-paper technology used in this work. (a) Xerox ColorQube 8570 printer; (b) solid ink (wax) cartridges; (c) SEM image of the surface of paper Whatman no. 1 with (green layer) and without printed solid ink (encapsulation); (d) optical micrographs of the paper cross section before and after diffusion of the wax through the entire paper thickness. In order to highlight the effect of the hydrophobic barriers a red dye solution was used.

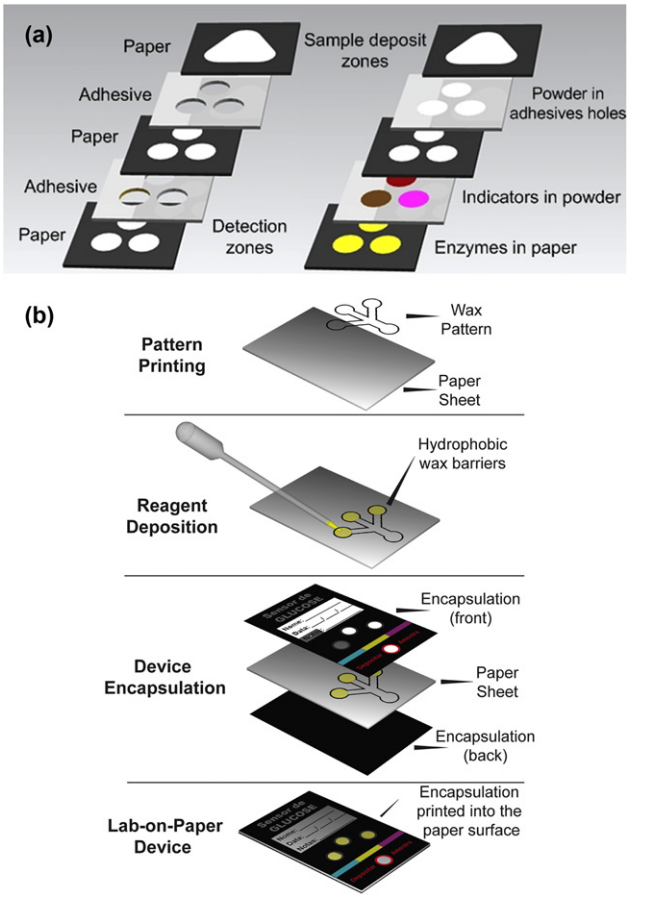

Figure 7. Illustration of the steps for paper-based device fabrication. (a) Wax-printed 3D devices composed of three layers of paper and two layers of adhesive tape. The holes in the adhesive tape are filled with cellulose powder allowing the contact between the adjacent layers. Each hole of the bottom adhesive contains a distinct indicator reagent (represented by distinct colours). For the purpose of glucose detection and quantification a solution of glucose oxidase and peroxidase enzymes is spotted onto the last layer of paper (represented by the yellow colour)—see text for explanation. (b) Fully enclosed 2D lateral flow devices.

coating the device with solid ink or toner layers. The entire device is made of biodegradable materials, with a considerably reduced volume, comparable to a paper sheet, which in turn reduces the transportation and storing costs of the final product. Furthermore, paper-based sensor disposal may be considered minor when compared with that of most rapid tests currently available, in which plastic polymer casings increase significantly the cost and the environmental impact.

In order to optimize the lab-on-paper technology, namely the wax-printing process, we have performed a set of experiments in terms of the time and temperature needed to melt the printed wax on the paper, to produce impermeable barriers across its entire thickness. Figure 8 shows the yield (working devices/total devices) as a function of temperature for two different time intervals. The results show that a 100% yield is reached for temperatures higher than 120 °C for both time intervals. For the work presented in this paper we have selected a temperature of 140 °C and a time interval of 2 min for the diffusion process, in order to guarantee the full operation of all the devices in terms of the impermeability of the wax barriers.

4. Proof-of-concept applications

4.1. Lab-on-paper for glucose measurement

Glucose is the primary energy source of cells, being transported through the bloodstream of organisms. The normal level of glucose in human blood is around 5.5 mM. This level may change during the day, being lower before meals and reaching a peak after these. Prolonged glucose levels outside the normal range may indicate the presence of a health condition, such as diabetes. We are working on a proof-of-concept 3D paper-platform that will ultimately allow the measurement of glucose levels in human blood and other biological fluids. The detection and quantification of glucose is based on enzymatic reactions. Briefly, the action of glucose oxidase decomposes glucose into hydrogen peroxide that is then utilized by a second enzyme, peroxidase. Peroxidase is responsible for the oxidation of colorimetric indicators generating a visible colour change. The colorimetric response is proportional to the initial amount of glucose in the sample. The fabrication of these wax-printed 3D biosensors is illustrated in figure 7(a). The device's assembly is based on the adhesion of layers of paper interspersed with layers of adhesive tape. The holes shaped in the adhesive are filled with cellulose powder to ensure a smooth contact between adjacent layers. An enzyme solution containing glucose oxidase, peroxidase and trehalose, used as a stabilizing agent, was spotted in

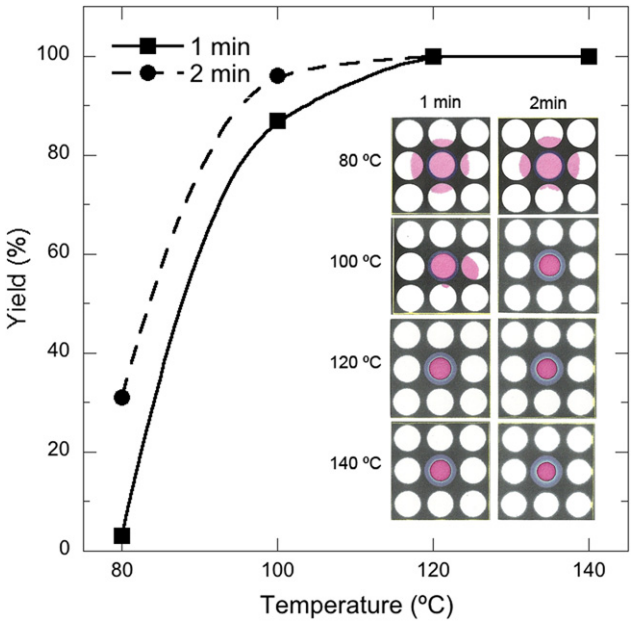

Figure 8. Yield as a function of temperature for two diffusion time intervals. The inset shows the optical image of the tested devices (96-well paper microplates). When the wax barriers are not completely impermeable after the diffusion process, the pink dye solution deposited in the central well overflows into the adjacent wells.

the three detection areas of the biosensor (figure 7(a)). After drying, a layer of adhesive tape filled with cellulose powder was glued. Different redox indicators were added to the cellulose powder in each of the three distinct holes: AB (4-aminoantipyrine + 3,5-dichloro-2-hydroxybenzenesulfonic acid), KI (potassium iodide), and a mixture of AB + KI (figure 7(a)).

To calibrate the biosensor response, solutions with increasing molar concentrations of glucose in sodium phosphate buffer were tested (0.01–100 mM). The results were assessed visually, and digitally where the RGB channel intensity was determined with the software Image J. The two paper-based formats developed for glucose sensing (lateral flow 2D and 3D) were compared in terms of sensitivity, which is related to colour uniformity. The results obtained in the proof-of-concept assays are illustrated in figure 9.

The test runs in less than five minutes and the intensity of the colour developed in each reaction zone increases with the concentration of the glucose solution tested. We can print a calibration colour gradient scale directly on the paper device in order to compare with test results, allowing us to infer an approximate concentration of glucose in the sample. Additionally, the colouration is highly homogeneous, covering all the surface of the paper reaction zones in 3D sensors, which is a major advantage in comparison to the previously described 2D lateral flow sensors, where some carryover of the coloured products usually occurs (figure 9(c)). The analysis is thus facilitated and is much more accurate. The indicator AB allows a visual distinction between 0.1 and 5 mM glucose concentrations. In the case of the KI indicator, a colorimetric change is visible in the 1–20 mM glucose concentration range, spanning most of the glucose concentrations of biological clinical interest (figure 9). The mixture of indicators AB + KI behaves as the individual indicators AB and KI, depending on the glucose concentration range. The use of multiple indicators with different sensitivities in the same test allows the interpretation of colorimetric results in a wide range of glucose concentrations, with greater accuracy. The results obtained by analysing the RGB channels of scanned tests are illustrated in figure 9. The green channel showed the highest intensity for the AB indicator, presenting colour saturation for glucose concentrations above 5 mM (figure 9(a)). Up to this concentration, the slope of the curve representing the variation in the intensity of the green channel as a function of glucose concentration is accentuated, which translates into a high sensitivity at low concentrations. This behaviour is also verified by visual analysis of the results (figure 9(c)). For the KI indicator, the blue channel was the one that showed the highest intensity (figure 9(b)). For glucose concentrations smaller than 5 mM this indicator shows a lower sensitivity than the AB. The colour saturation of the KI indicator occurs for glucose concentrations above 40 mM.

The results obtained with the above-described proof-of-concept 3D glucose sensors are thus promising towards the future of simple and cost-effective paper-based devices.

4.2. Lab-on-paper for the detection of anti-Leishmania antibodies in sera

Visceral leishmaniasis is a severe sand-fly transmitted zoonotic disease caused by protozoan parasites *Leishmania donovani* (in East Africa and the Indian subcontinent) and *Leishmania infantum* (in Latin America and the Mediterranean basin) (figure 10). Dogs constitute the main host reservoir of *Leishmania* agents and the disease is endemic in the Mediterranean basin, the Middle East and several tropical regions. Canine leishmaniasis ranges from cutaneous to systemic forms and a fatal course is often associated with renal damage. An early diagnosis of this disease in dogs is essential for surveillance and control programs. The disease is routinely diagnosed in veterinary settings using immunological-based approaches, and detection of specific-antibodies against *Leishmania* parasites remains the method of choice for mass screening of dogs in epidemiological surveys [23]. Among the different tests available, the most widely used are immunofluorescent-antibody tests (IFATs), direct agglutination tests (DATs) and 96-well enzyme-linked immunosorbent assays (ELISAs) [23]. Most of these tests rely on the use of antigen fractions of the promastigote/amastigote stages of *Leishmania* parasites or on a recombinant highly conserved antigen (rK39) [23, 24].

We briefly describe the assembly of a proof-of-concept paper-based ELISA platform for the detection of anti-*Leishmania* antibodies in canine sera. Promastigotes of an *L. infantum* reference strain were used to produce antigens to detect anti-*Leishmania* antibodies. Parasites were collected from one-week cultures by centrifugation and the washed

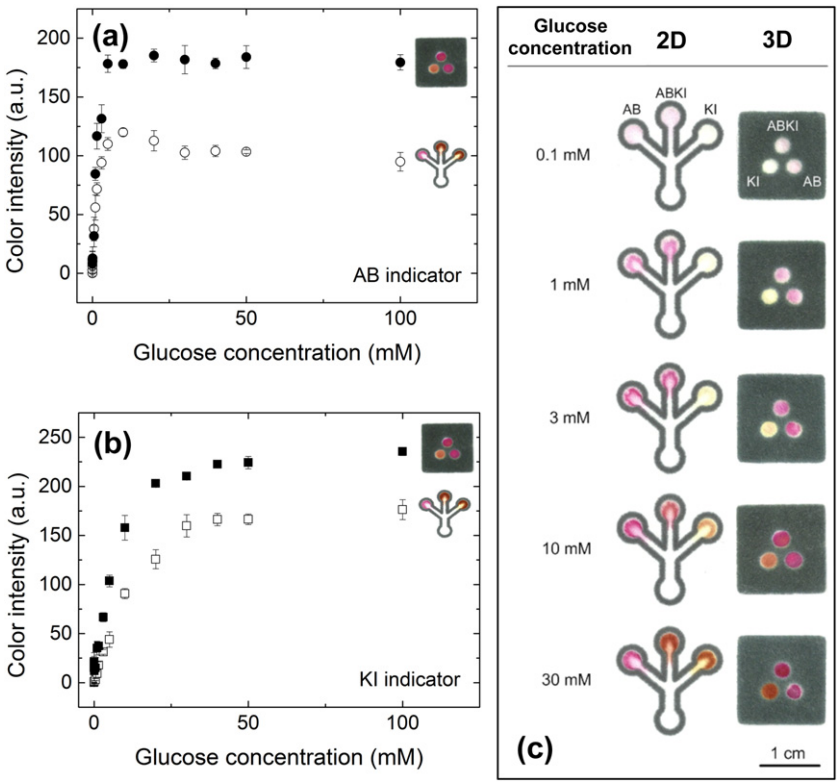

Figure 9. Comparison between lateral flow 2D and 3D glucose sensors. (a) Graphical representation of the colour intensity of detection zones containing the AB indicator when tested with increasing concentrations of glucose (filled and empty circles correspond to the 3D and lateral flow 2D sensors, respectively); (b) graphical representation of the colour intensity of detection zones containing the KI indicator when tested with increasing concentrations of glucose (filled and empty squares correspond to the 3D and lateral flow 2D sensors, respectively); (c) colorimetric results obtained with two formats of paper-based glucose sensors when tested with increasing concentrations of glucose solutions (0.1–30 mM): the format on the left corresponds to the lateral flow 2D glucose sensor and on the right corresponds to the described 3D sensor.

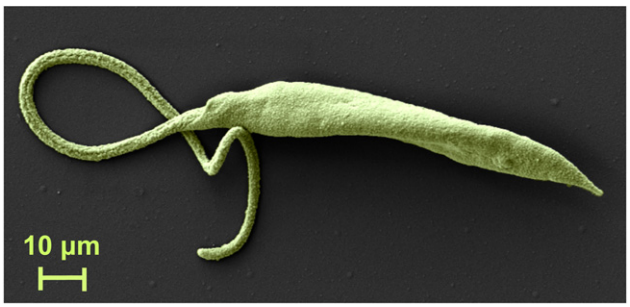

Figure 10. SEM (Carl Zeiss Auriga Crossbeam SEM-FIB) image of a glutaraldehyde fixed *Leishmania infantum* promastigote.

pellets were suspended in water, sonicated and high-speed centrifuged. After quantification of the crude proteins, the supernatant was used as the antigen solution (concentration adjusted to 1 μg μl^{-1}). This antigen solution was spotted in the wells of the paper-platform and, after drying, the wells were impregnated with blocking buffer (containing bovine serum albumin) in order to block any posterior nonspecific interactions with cellulose fibers. After a drying process at ambient conditions, the test was performed as illustrated in figure 11.

The occurrence of antibody–antigen biorecognition events was flagged using commercially available anti-dog secondary antibodies conjugated with alkaline-phosphatase and the substrate BCIP/NBT (similarly to simple conventional ELISA assays). Briefly, a dilution (1:10) of a dog serum sample was added to a well of the paper-platform (where *Leishmania* antigens were previously immobilized) (figure 11). After a 15 min incubation period, the well was washed with phosphate buffer and an alkaline phosphatase-conjugated secondary antibody was added. This secondary antibody has affinity for the conserved part of the dog antibodies and will therefore bind any anti-*Leishmania* antibodies immobilized by the antigens. After a 10 min incubation period and novel washing steps, the BCIP/NBT substrate was added to the well. If the dog serum contains anti-*Leishmania* antibodies, a blue colour develops on the paper surface as a result of the degradation of BCIP/NBT by the alkaline–phosphatase (figure 11). All test procedures take less than 60 min (including the incubation periods). Following colour development, the paper platforms were scanned and digital images were analysed with Image J software. Using the selection tool, a circle containing the entire area of a well was drawn and the average of the RGB channels in the selected area was recorded. Figure 12 illustrates the results obtained using sera from two dogs, one infected with canine leishmaniasis

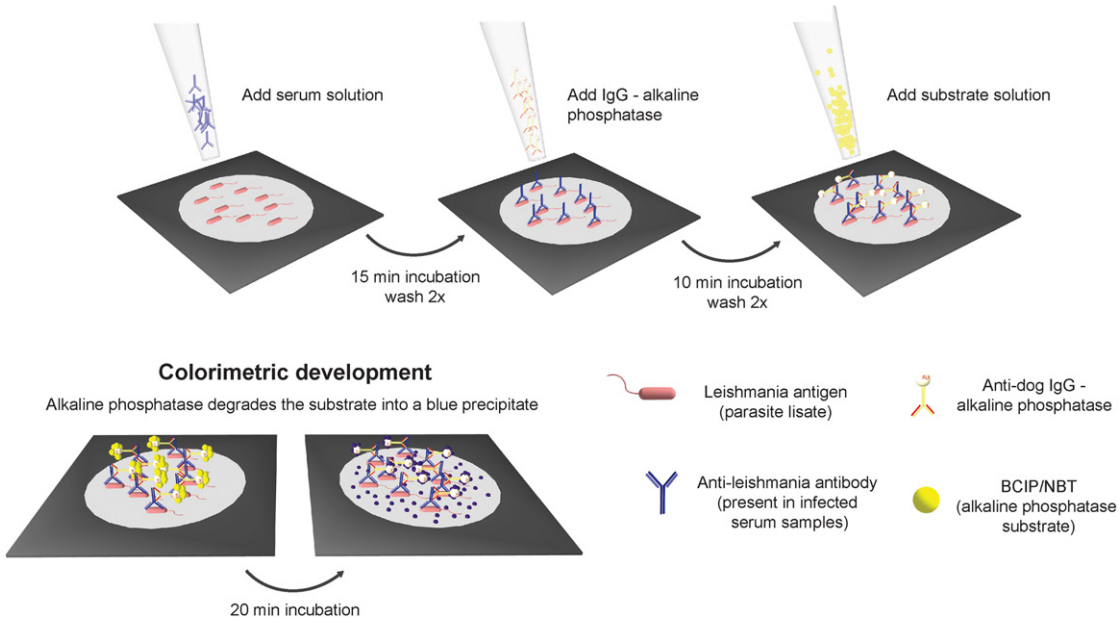

Figure 11. Schematic representation of the paper-based ELISA assay developed for the diagnosis of canine leishmaniasis. The test allows the colorimetric detection of anti-*Leishmania* antibodies in canine sera (the several steps are illustrated for a single well—see the text for explanation).

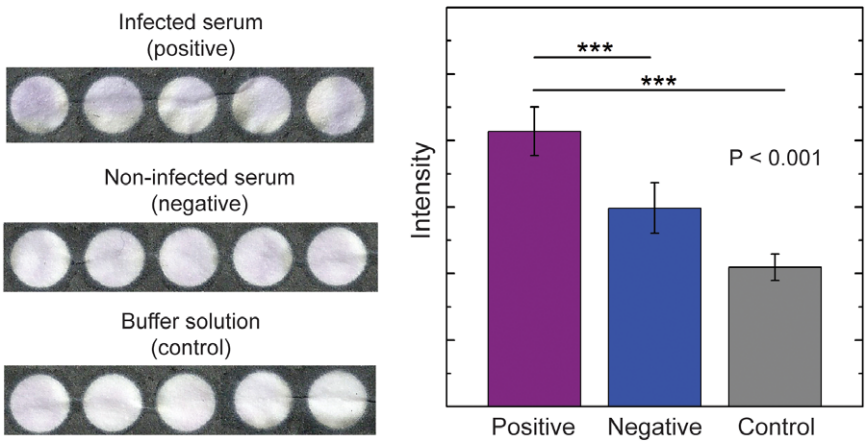

Figure 12. Paper-based 96-well ELISA assay for the detection of anti-*Leishmania* antibodies in canine sera. Left: colorimetric results of the test performed with serum from an infected and a non-infected animal, and a negative control. Right: graphical representation of the colour intensity corresponding to positive, negative and control wells, determined after image analysis of the scanned paper-platform. The bars represent the average of five independent measurements and the error bars indicate the standard deviation. Statistical analysis was performed using Prism 5 Graph Pad, using one-way ANOVA with Tukey's multiple comparison test; $^{***} = p < 0.001$, $n = 5$.

and another non-infected. The control solution contained only serum dilution buffer.

A small variation in colour intensity was visually observed between the three sets of wells (positive, negative and control test) (figure 12). Still, the wells where an infected serum was deposited presented a significantly darker blue colouration than the negative and control wells. This result suggests that the anti-*Leishmania* antibodies in the infected serum attached to the paper-immobilized antigens. Digital analysis of the scanned tests allowed the determination of the colour intensity corresponding to each well. There was a statistically significant difference between the set of wells corresponding to a positive test in relation to the negative and control tests (figure 12). At a conceptual level this paper-based device shows therefore very promising results. Nevertheless, future optimization is still needed, namely in the selection of more efficient and specific *Leishmania* antigens, such as the purified recombinant *Leishmania* rk39 antigen, and in their immobilization techniques in cellulose fibres.

4.3. Lab-on-paper for the detection of Mycobacterium tuberculosis

Tuberculosis (TB) is a leading cause of morbidity and mortality in the world, also affecting a wide range of animal species, particularly livestock, in both developed and developing countries. The disease is caused by bacteria belonging

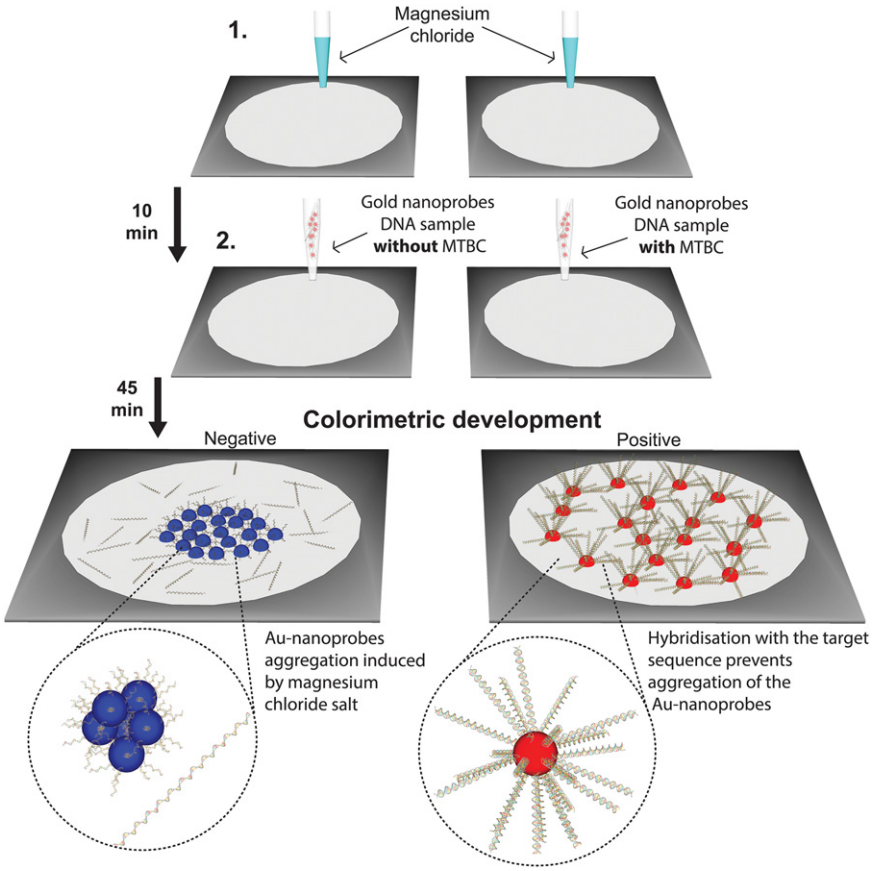

Figure 13. Illustration of the paper-based application to specifically detect MTBC nucleic acids after hybridization with species-specific gold-nanoprobes (the several steps are illustrated for two wells of the paper-platform, yielding a positive and a negative result—see the text for explanation).

to the *Mycobacterium tuberculosis* complex (MTBC) that encompasses closely-related pathogenic species, namely *M. tuberculosis*, the main agent of human TB, *M. bovis* and *M. caprae*, associated to bovine and caprine TB, respectively, among others. *Mycobacterium bovis* and *M. caprae* also represent a high potential for zoonotic transmission to humans. Conventional laboratory diagnosis of TB in both human and veterinary settings is lengthy, cumbersome and does not routinely differentiate between MTBC species. Rapid and accurate laboratory tests for the direct detection and/or identification of MTBC species are in high demand and are crucial for improved TB control. In this framework, our group recently disclosed a proof-of-concept paper-based application to specifically detect MTBC nucleic acids after hybridization with species-specific gold (Au)-labelled oligonucleotide probes (Au-nanoprobes) [11]. The Au-nanoprobe is complementary to a region of the RNA polymerase beta subunit locus able to specifically identify MTBC members, and the assay is processed on a paper-platform (figure 13). Briefly, this paper-platform consisted of a wax-printed 384-well plate, which was impregnated with a pre-determined concentration of salt ($MgCl_2$) capable of inducing Au-nanoprobe aggregation [11]. The assay relies on the mixing between the Au-nanoprobe and the target DNA sequence from the putative MTBC isolate, which may be previously amplified by standard polymerase chain reaction (figure 13). In this non-cross-linking assay, the Au-nanoprobe/target DNA mixture is added to a well of the 384 salt-impregnated paper-based plate, which keeps a red colour. After incubation for some minutes, aggregation of Au-nanoprobes is induced by the salt but the presence of an MTBC-specific complementary target prevents Au-nanoprobe aggregation and the paper surface remains red; absence of a complementary MTBC target does not prevent Au-nanoprobe aggregation, which results in a visible colour change from red to blue in the paper surface (figures 13 and 14).

A simple colorimetric analysis of hybridization results allows therefore the identification: the presence of an MTBC species yields a red colour while a blue colour means a negative result for the identification of any TB-causing mycobacteria (figure 14). The whole process, including the PCR amplification step, takes less than 2 h 30 min, which is considerably faster than traditional methods [11]. Because of the paper's white background, the colour contrast is greatly improved without the need for expensive reagents. In addition to the simple colorimetric assessment of non-cross-linking hybridization results, the integration of the paper-platform with a smartphone and a simple data analysis tool allowed the quantification of the colorimetric changes on the paper (figure 14) [11].

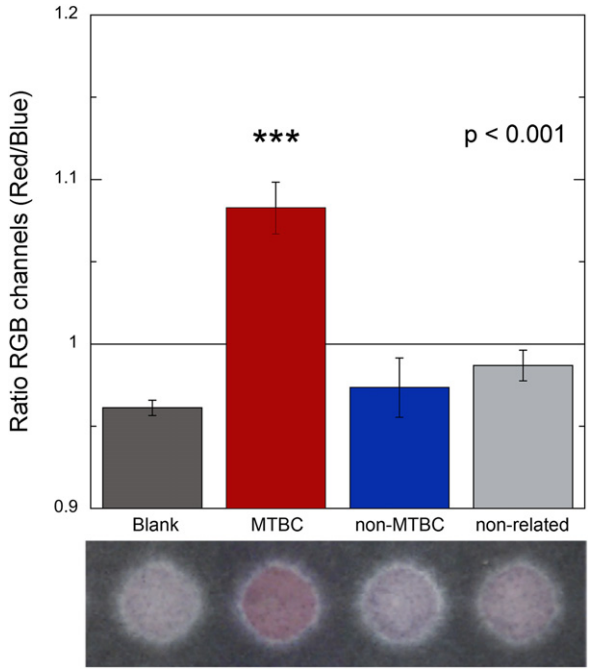

Figure 14. Au-nanoprobe assay for MTBC detection performed in the paper microplate (adapted from Veigas *et al* [11]). Top: nanoprobe aggregation as measured by digital RGB analysis. Ratio of aggregation calculated in a smartphone (ratio of average intensity of the Red and Blue channels) for the assay mixtures. The bars represent the average of three independent measurements and the error bars indicate standard deviation. The horizontal line represents the threshold of 1 considered for discrimination between positive and negative. Statistical analysis was performed using Prism 5 Graph Pad, using one-way ANOVA with Tukey's multiple comparison test; $^{***} = p < 0.001$, $n = 3$. Bottom: photo of the paper plate captured after colour development, corresponding to the wells of a positive reaction (MTBC) and controls (blank, non-MTBC and non-related).

In work carried out after the publication of the above-mentioned paper from Veigas and colleagues [11], an energy-dispersive x-ray spectroscopy analysis was performed on a well of the paper-platform corresponding to a negative result for the presence of MTBC, in order to obtain an elemental analysis of the sample (figure 15). The SEM image shows an aggregate of Au-nanoprobes on the surface of a cellulose fibre. In the EDS maps corresponding to the SEM image, we can detect the carbon and oxygen elements, resulting from the composition of the cellulose fibre where the gold is deposited. The detectors also revealed the presence of considerable amounts of chlorine and magnesium, a result of the impregnated salt ($MgCl_2$) solution in the paper to induce aggregation of gold nanoparticles. Finally, the EDS distribution map also allows the detection of the gold element in the sectors of the cellulose fibre where aggregation of Au-nanoprobes occurred, corresponding to a negative result of the non-cross-linking hybridization test (figure 15).

Future studies will be carried out to simplify the paper-platform assay, by the elimination of the polymerase chain reaction step, which depends on the use of thermocycler equipment, and its replacement by an undemanding isothermal DNA amplification such as LAMP [25]. This isothermal DNA amplification step will also be integrated in the paper-platform assay. The assay will be optimized towards the direct detection of MTBC species in clinical samples, and to extend the range of applications to the screening of mutations associated with drug resistance.

5. Conclusions

Rapid tests have become quite common in developed countries as complementary diagnostic methods, a good example being the common pregnancy test. Despite their simplicity, most of these tests have high manufacturing costs, limiting their broader use in regions that are economically and socially underprivileged. Current research aims to provide cheaper, portable and yet robust diagnostic platforms to be used in low-resource settings, without specialized infrastructures. In this context lab-on-paper technology is being explored, also by our group, towards the development of low-cost and easy-to-use diagnostic biosensors. These sensors are likely to

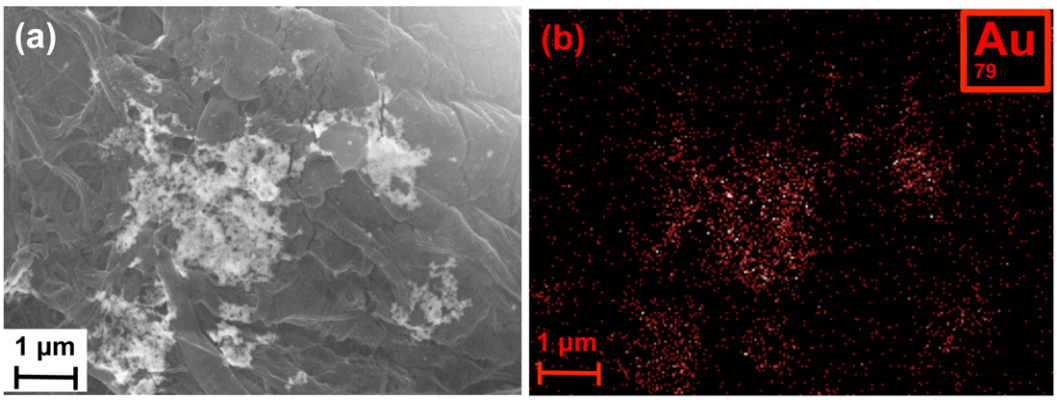

Figure 15. SEM image of a well corresponding to a negative result of the paper-platform used for detecting MTBC nucleic acids, where gold aggregates formed (a) and respective Energy-Dispersive x-ray Spectroscopy analysis showing the presence of the gold element (b).

be adapted to the detection of numerous compounds, such as drugs, hormones, enzymes, nucleic acids or biological markers of disease. In the future such devices will complement the diagnosis and/or allow monitoring therapies. In addition to the development of diagnostic devices, lab-on-paper technology may also be promising in other relevant contexts, such as food quality and environmental control.

Acknowledgments

This work has been financed by the European Commission under projects INVISIBLE (FP7 ERC AdG no 228144) and APPLE (FP7-NMP-2010-SME/262782-2), and the Portuguese Science Foundation (FCT-MEC) through the Projects PEst-C/CTM/LA0025/2013-14, EXCL/CTM-NAN/0201/2012, PEst-C/CTM/LA0025/2011, PEst-OE/SAU/UI0009/2011, PTDC/CVT/111634/2009, PTDC/CTM/NAN/109877/2009. Mafalda Costa and Bruno Veigas were supported by FCT/MEC (SFRH/BD/90891/2012 and SFRH/BD/78970/2011, respectively).

The authors would like to thank their colleagues Daniela Nunes and Sónia Pereira, for the SEM and XRD, respectively.

References

[1] Martinez A W, Phillips S T, Whitesides G M and Carrilho E 2010 *Anal. Chem.* **82** 3–10
[2] Nygaard A P and Hall B D 1963 *Biochem. Biophys. Res. Commun.* **12** 98–104
[3] Pelton R 2009 *TRAC Trends Anal. Chem.* **28** 925–42
[4] Vella S J, Beattie P, Cademartiri R, Laromaine A, Martinez A W, Phillips S T, Mirica K A and Whitesides G M 2012 *Anal. Chem.* **84** 2883–91
[5] Martinez A W, Phillips S T, Butte M J and Whitesides G M 2007 *Angew. Chem. Int. Edn* **46** 1318–20
[6] Carrilho E, Martinez A W and Whitesides G M 2009 *Anal. Chem.* **81** 7091–5
[7] Martinez A W, Phillips S T and Whitesides G M 2008 *Proc. Natl Acad. Sci.* **105** 19606–11
[8] Schilling K M, Lepore A L, Kurian J A and Martinez A W 2012 *Anal. Chem.* **84** 1579–85
[9] Zhao W, Ali M M, Aguirre S D, Brook M A and Li Y 2008 *Anal. Chem.* **80** 8431–7
[10] Abe K, Kotera K, Suzuki K and Citterio D 2010 *Anal. Bioanal. Chem.* **398** 885–93
[11] Veigas B, Jacob J M, Costa M N, Santos D S, Viveiros M, Inácio J, Martins R, Barquinha P, Fortunato E and Baptista P V 2012 *Lab Chip* **12** 4802–8
[12] Lu J, Ge S, Ge L, Yan M and Yu J 2012 *Electrochim. Acta* **80** 334–41
[13] Araújo A C, Song Y, Lundeberg J, Stahl P L and Brumer H 2012 *Anal. Chem.* **84** 3311–7
[14] Su S, Ali M M, Filipe C D M, Li Y and Pelton R 2008 *Biomacromolecules* **9** 935–41
[15] Southern E M 1975 *J. Mol. Biol.* **98** 503–8
[16] Tonkinson J L and Stillman B A 2002 *Front. Biosci.* **7** c1–c12
[17] López-López M, de la Ossa M A F, Galindo J S, Ferrando J L, Vega A, Torre M and García-Ruiz C 2010 *Talanta* **81** 1742–9
[18] Tse H Y and Wong R C 2009 *Lateral Flow Immunoassay* (Totowa, NJ: Springer)
[19] Fridley G E, Holstein C A, Oza S B and Yager P 2013 *MRS Bull.* **38** 326–30
[20] Bhushan B and Jung Y C 2011 *Prog. Mater. Sci.* **56** 1–108
[21] Ensikat H J, Ditsche-Kuru P, Neinhuis C and Barthlott W 2011 *Beilstein J. Nanotechnol.* **2** 152–61
[22] Segal L, Creely J J, Martin A E and Conrad C M 1959 *Text. Res. J.* **29** 786–94
[23] Mettler M, Grimm F, Capelli G, Camp H and Deplazes P J 2005 *Clin. Microbiol.* **43** 5515–9
[24] Takagi H, Islam M Z, Itoh M, Islam A U, Saifuddin Ekram A R M, Hussain S M, Hashiguchi Y and Kimura E 2007 *Am. J. Trop. Med. Hyg.* **76** 902–5
[25] Notomi T, Okayama H, Masubuchi H, Yonekawa T, Watanabe K, Amino N and Hase T 2000 *Nucleic Acids Res.* **28** e63